

Spatiotemporal Pattern Modulations in the Taylor-Dean System

Innocent Mutabazi,^(a) John J. Hegseth, and C. David Andereck

Department of Physics, Ohio State University, 174 West 18th Avenue, Columbus, Ohio 43210

Jose E. Wesfreid

*Laboratoire d'Hydrodynamique et Mécanique Physique,
Ecole Supérieure de Physique et de Chimie Industrielles de Paris, 10, rue Vanquelin,
75231 Paris CEDEX 05, France*

(Received 1 December 1989)

Flow between two horizontal coaxial cylinders with a partially filled gap is investigated for the case when the primary instability forms a pattern of traveling inclined rolls which is simply periodic in space and time. Slightly above the onset, there is a second instability which results in a periodic modulation of the rolls with an axial wavelength of ~ 3 rolls and a lower frequency. Both the traveling inclined rolls and the ~ 3 -roll-modulation pattern exhibit long-wavelength, low-frequency phase modulations and associated defects.

PACS numbers: 47.20.-k

The transition to turbulence remains one of the major problems of nonlinear physics which is still not well understood. In the last few years, considerable effort has been devoted to the problem of the formation of cellular patterns, and their subsequent evolution to disorder, in fluid systems far from equilibrium such as Rayleigh-Bénard convection and Taylor-Couette flow, as well as many other hydrodynamic, mechanical, and physico-chemical systems.^{1,2} In such cases, the bifurcation from the base state occurs via a stationary or an oscillatory instability (Hopf bifurcation). Recently, attention has been drawn to systems in which the transition from the base state occurs via a Hopf bifurcation, in which case the transition to spatial-temporal complexity may be more accessible for experimental characterization and theoretical treatment. Such systems include convection in binary mixtures³ and in liquid crystals,⁴ the Taylor-Couette system with counter-rotating cylinders,⁵ the Taylor-Dean system,⁶ chemical reactions,^{7,8} and plastic deformation with negative-strain-rate sensitivity.⁹

We report the first observation of an unusual transition sequence in the behavior of a hydrodynamic system with well controlled centrifugal instabilities, the Taylor-Dean system. The system consists of flow between two horizontal coaxial rotating cylinders with a partially filled gap. The flow patterns observed depend on the inner- and outer-cylinder rotation speeds, which we rescale as our dimensionless control parameters, the inner- and outer-cylinder Reynolds numbers R_i and R_o . Depending on the value of R_o selected, the flow evolves upon increasing R_i to either a stationary axisymmetric-roll pattern or a traveling-inclined-roll pattern (Hopf bifurcation).⁶ We investigate here the behavior of the traveling-roll pattern when the outer cylinder is at rest and R_i is slowly increased. Just above the onset, a phase variation in the pattern produces a long-wavelength modulation and time-dependent pattern defects are gen-

erated. At higher rotation speeds, the pattern undergoes an unusual periodic short-wavelength amplitude modulation with an envelope size of ~ 3 rolls. While investigation of different extended one-dimensional systems with a Hopf bifurcation as the first transition has led to interesting results such as solitary-wave-like behavior¹⁰⁻¹² or isolated patches of traveling rolls,¹³⁻¹⁶ we know of no other system with traveling patterns at onset which undergoes such a short-wavelength modulation. The aim of this Letter is to present the main characteristics of this novel traveling pattern, and describe its evolution toward spatial-temporal complexity.

The Taylor-Dean system may be understood (and distinguished from the Taylor-Couette system) by observing that the partial filling of the gap between the cylinders produces two horizontal surfaces. When the cylinders rotate they drive the fluid toward a free surface. To reverse the direction of the flow the free surface induces a pressure gradient along the azimuthal direction (Fig. 1). As a result, the flow sufficiently far away from the free surfaces can be regarded as a combination of Couette flow, from the rotation of the cylinders, and Poiseuille flow, due to the azimuthal pressure gradient. The traveling-roll pattern may then arise as a result of the competition between centrifugal instabilities of the Couette and Poiseuille components of the flow.¹⁷

Our system consists of two horizontal coaxial cylinders, the inner cylinder made of black Delrin plastic with an outer radius $r_o = 4.486$ cm and the outer cylinder made of Duran glass with an inner radius $r_i = 5.080$ cm. The gap between the cylinders is $d = r_o - r_i = 0.594$ cm and the cylinders are independently driven as described elsewhere.⁶ The radius ratio $\eta = 0.883$ is large enough for the small-gap approximation to be reasonable. Teflon rings are attached to the inner surface of the outer cylinder a distance $L = 53.40$ cm apart, giving an aspect ratio $\Gamma = L/d = 90$. The fluid is water with 1%

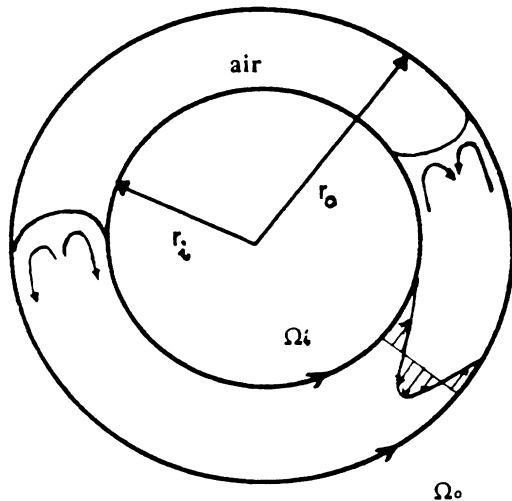


FIG. 1. Sketch of the experimental geometry: Corotating cylinders with a partially filled gap. The front face is defined to be the one in which the inner cylinder is rotating upward.

Kalliroscope AQ1000 for visualization. We have fixed the filling-level fraction $n = \theta_f / 2\pi$ at 0.75.⁶ (The instability threshold depends only weakly on n . For $n \in [0.5, 0.8]$ the variation of R_{ic} is within the experimental precision ($\approx 1\%$).

We define inner- and outer-cylinder Reynolds numbers as follows: $R_i = 2\pi f_i r_i d / \nu$ and $R_o = 2\pi f_o r_o d / \nu$, respectively, where f_i and f_o are the inner- and outer-cylinder rotation frequencies. The dimensionless control parameter is $\epsilon = (R_i - R_{ic}) / R_{ic}$, where R_{ic} is the inner-cylinder Reynolds number at onset of the traveling inclined rolls for a given R_o . The flow-pattern frequencies are scaled with the inverse of the radial diffusion time $\tau_r = d^2 / \nu \approx 36$ s, the wavelengths are scaled by the gap size d , and the velocities are scaled by the radial diffusion velocity ν/d .

Frequency measurements at a single position in the flow have been made by the light-reflectance technique described elsewhere.⁶ Spatial information is obtained using a 28–35-mm variable-focal-length lens to image the flow pattern onto a 1024-pixel charge-coupled-device (CCD) linear array. The array is controlled by a CAMAC module, which also serves as the data gateway to our PDP-11 computer. This system is able to continuously process up to one frame every 0.07 s. The output of the CCD camera gives the instantaneous reflected light intensity along the axis of the cylinders, the maxima corresponding to roll centers and the minima corresponding to inflow and outflow boundaries. Space-time diagrams are then produced by displaying intensity versus axial position plots at regular intervals along a time axis. We have also used a high-intensity white-light source to illuminate a thin cross section of the flow to visualize the internal processes in the structures.

The initial instability to traveling rolls is, within our

experimental limits, a supercritical Hopf bifurcation. The intensity of the rolls decreases along the azimuth such that they are weaker in the rear face than in the front face. This may be connected to the presence of a horizontal recirculation roll at the front free surface. The rolls are inclined $\sim 20^\circ$ from the vertical (Fig. 2). The wavelength of the rolls along the cylinders' axis is $\lambda = 1.416$. At onset the rolls have no preferred direction and may move either left or right. The direction of propagation is the same as the roll inclination direction. Light sheet visualization through the gap shows that the rolls exist near the outer cylinder. Above threshold both right- and left-traveling rolls may exist separated by a vertical (noninclined) defect line. The defect line is not necessarily in the middle of the cylinder axis; in fact, it moves in an erratic fashion with a velocity of about 50 times less than that of the rolls. Such defect lines are inherent to traveling-wave patterns.¹⁸

We have measured the frequencies of the traveling rolls (from power spectra) as a function of R_i , as shown in Fig. 3. Near the onset, for a fixed R_o , the fundamental frequency f of the traveling rolls increases almost linearly with R_i . Measurements of the frequency at different points along the axis show that for $\epsilon \approx 0.013$, and above, there is a local frequency of the pattern. This can also be seen in Fig. 2 where the phase lines of the rolls are curved. Close to onset, after either a left- or right-traveling roll pattern has grown to a length of ~ 30 rolls, a long-wavelength modulation appears which generates this phase variation. The wavelength of this modulation decreases from ~ 30 to ~ 10 rolls as R_i increases. For $\epsilon \in [0.02, 0.1]$ the frequency and roll-velocity variation becomes strong. High-velocity rolls occasionally collide with low-velocity rolls, resulting in the loss of a roll. The collision gives rise to a damped modulation moving in a direction opposite to the traveling rolls. Roll creation events have also been observed [as can be deduced from Fig. 2(a)]. Similar roll creation and destruction events have been observed in binary-fluid convection¹⁴ and in electrohydrodynamic systems.¹⁹

Increasing R_i , the flow undergoes a second instability which results in a short-wavelength modulation of the traveling waves [Fig. 2(b)]. The onset is nonhysteretic, within our experimental precision of $\approx 1\%$. It manifests itself as a roll-intensity modulation with a nonsymmetric envelope of wavelength $\Lambda = 4.11$ and lower frequency f_2 of about 0.7 for $R_o = 0$. The size of an individual roll changes as it travels through the modulation envelope. This ~ 3 -roll (short-wavelength) modulation appears for $-45 < R_o < 45$ with a threshold varying as shown in Fig. 4. The modulation envelope moves with a velocity depending on the value of R_o .

The short-wavelength modulations produce distortions of each roll along its axis [Fig. 2(b)]. This suggests that the short-wavelength modulation may be analogous to the wavy spirals in the counter-rotating Taylor-Couette system.⁵ Given the axial velocities in the data of Fig.

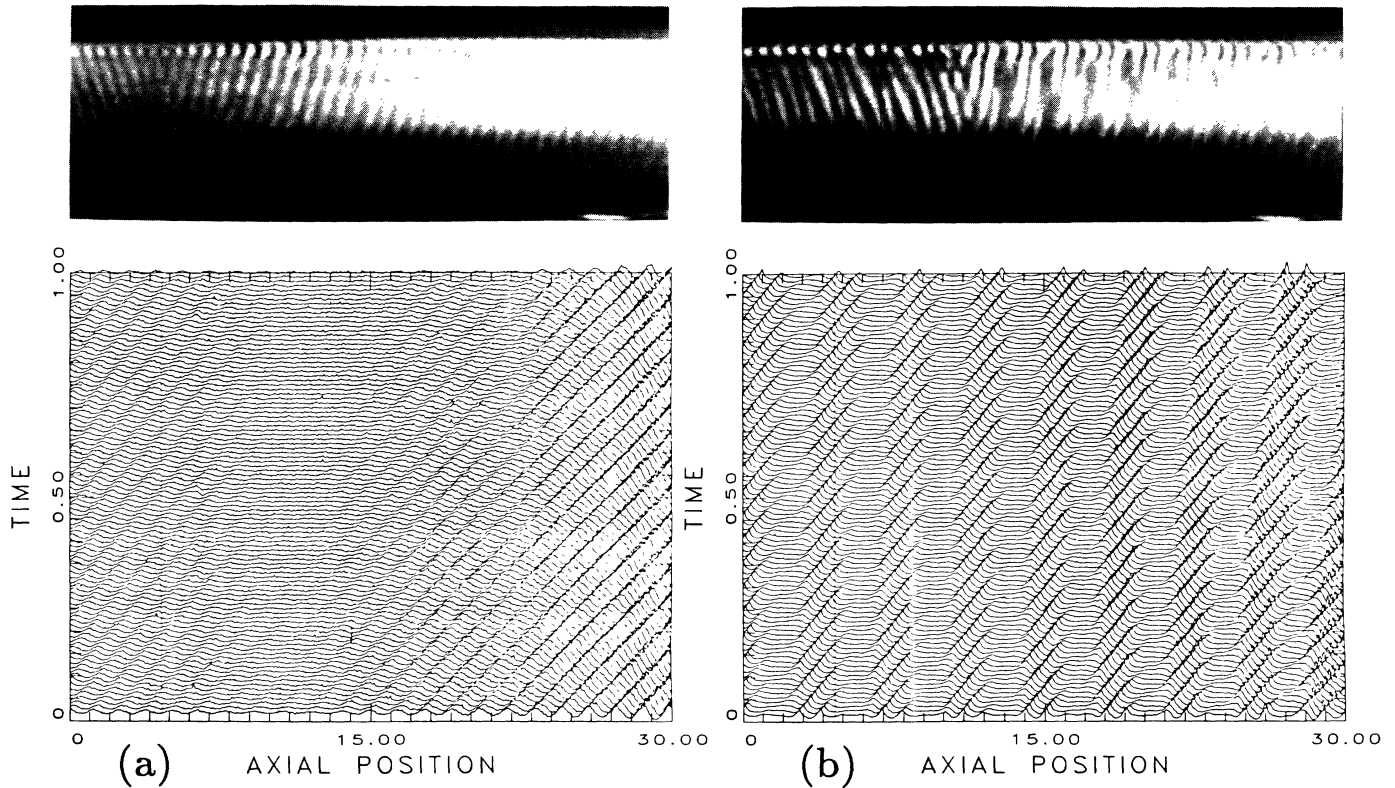


FIG. 2. Photographs of the traveling-roll patterns viewed from the front face (the top of each view being a free horizontal surface) and their space-time diagrams: (a) traveling-inclined-roll pattern near threshold at $R_i=263$ and $R_o=0$. (b) Short-wavelength (~ 3 -roll) -modulation pattern at $R_i=303$ and $R_o=0$.

2(b), and the 20° inclination angle, there should be ≈ 2.9 azimuthal waves. We observe ≈ 2 waves in the front face while the third may remain unseen because of the decreasing intensity of the rolls along the azimuth.

We measured the time-averaged spatial intensity-intensity correlation function of the rolls along the axis for $R_o=0$. Time averaging of individual spatial autocorrelations was done over a time of $\approx 40\tau$, and had the effect of removing the

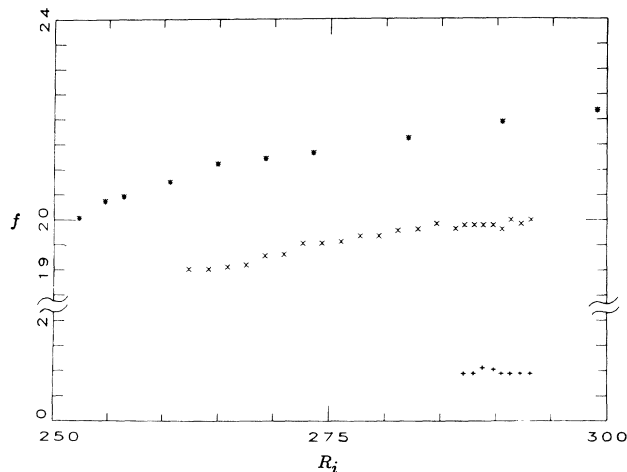


FIG. 3. Fundamental and secondary frequencies as functions of R_i : fundamental frequency for $R_o=0$ (\times), for $R_o=39$ ($*$), and the secondary frequency for $R_o=0$ ($+$).

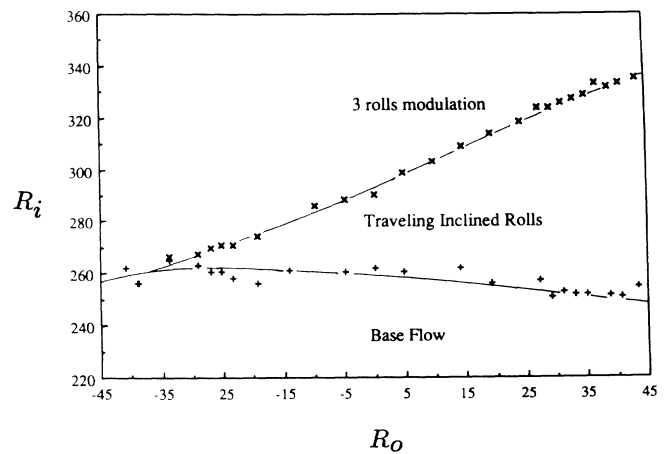


FIG. 4. Phase diagram (R_o, R_i) for the threshold of the inclined-traveling-roll pattern, and the short-wavelength-modulation pattern. The solid lines are guides to the eye.

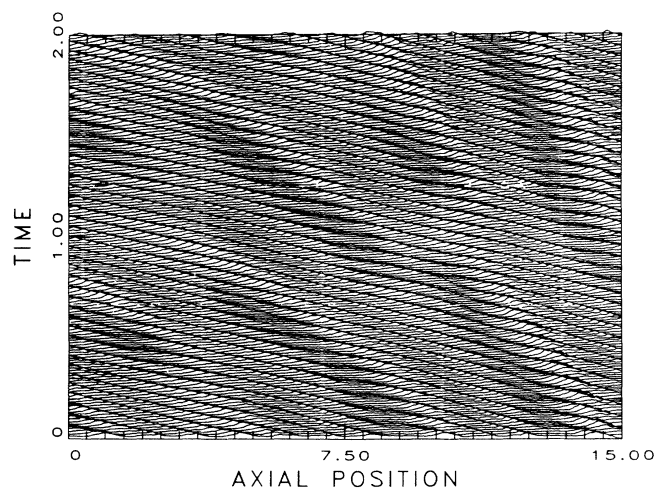


FIG. 5. The ~ 3 -roll pattern at $R_i = 308$, $R_o = 0$. The traveling rolls are separated by propagating envelopes which exhibit phase modulations and defects.

long-range correlation. Before the onset of the short-wavelength modulation, the envelope of this correlation function decreases smoothly within an exponential envelope with a characteristic length of about 2.6. After the short-wavelength modulation appears, the correlation remains strong only at distances of 3 rolls. This reflects the varying roll size and apparent strength within a modulation wavelength. This phenomenon can be considered as the generation of traveling patches (triplets) periodic in space and in time separated by periodic laminarlike zones. As in the case of the initial traveling-roll pattern, the roll-modulated pattern may exhibit spatiotemporal defects (Fig. 5). At these and higher R_i values the correlation function drops rapidly to zero beyond one roll wavelength.

To summarize, for a large-aspect-ratio Taylor-Dean system, the traveling inclined rolls observed at the onset of instability, undergo, after the onset of a long-wavelength modulation associated with defects, a novel short-wavelength modulation with an axial wavelength of ~ 3 rolls. This modulation may be generated either by competing instabilities in different layers or by a wavy instability of the rolls. This short-wavelength-modulation pattern strongly distorts individual rolls and exhibits a long-wavelength modulation associated with defects. This transition to the ~ 3 -roll-modulation pattern is not far from the onset of the primary instability, making this system a good candidate for investigating the transition to weakly turbulent states.

We thank Christiane Normand and Yves Pomeau for

interesting suggestions. I.M. thanks the staff of the Nonlinear Dynamics Laboratory for all that they provided him during his stay at Ohio State University. This work has been supported by the Office of Naval Research and NATO.

^(a)Present address: Laboratoire d'Hydrodynamique et Mécanique Physique, Ecole Supérieure de Physique et de Chimie Industrielles de Paris, 10, rue Vauquelin, F-75231 Paris CEDEX 05, France.

¹*Cellular Structures in Instabilities*, edited by J. E. Wesfreid and S. Zaleski, Lecture Notes in Physics Vol. 210 (Springer-Verlag, Berlin, 1984).

²*Propagation in Systems Far from Equilibrium*, edited by J. E. Wesfreid, H. R. Brand, P. Manneville, G. Albinet, and N. Boccara, Springer Series in Synergetics Vol. 41 (Springer-Verlag, Berlin, 1988).

³P. Kolodner and C. M. Surko, *Phys. Rev. Lett.* **61**, 842 (1988).

⁴I. Rehberg, S. Rasenat, and V. Steinberg, *Phys. Rev. Lett.* **62**, 756 (1989).

⁵C. D. Andereck, S. S. Liu, and H. L. Swinney, *J. Fluid Mech.* **164**, 155 (1986).

⁶I. Mutabazi, J. J. Hegseth, C. D. Andereck, and J. E. Wesfreid, *Phys. Rev. A* **38**, 4752 (1988).

⁷Y. Kuramoto, *Chemical Oscillations, Waves and Turbulence*, Springer Series in Synergetics Vol. 19 (Springer-Verlag, Berlin, 1984).

⁸Z. Nagy-Ungvarai and S. C. Müller, in *Propagation in Systems Far from Equilibrium* (Ref. 2), p. 100.

⁹Y. Estrin and L. P. Kubin, *Res Mech.* **23**, 197 (1988).

¹⁰M. Rabaud, S. Michalland, and Y. Couder, *Phys. Rev. Lett.* **64**, 184 (1990).

¹¹A. Simon, J. Bechhoefer, and A. Libchaber, *Phys. Rev. Lett.* **61**, 2574 (1988).

¹²G. Faivre, S. de Chivigné, C. Guthmann, and P. Kurowski, *Europhys. Lett.* **9**, 779 (1989).

¹³P. Kolodner, C. M. Surko, and H. Williams, *Physica (Amsterdam)* **37D**, 319 (1989).

¹⁴P. Kolodner, D. Bensimon, and C. M. Surko, *Phys. Rev. Lett.* **60**, 1723 (1988).

¹⁵R. Henrichs, G. Ahlers, and D. S. Cannell, *Phys. Rev. A* **35**, 2761 (1987).

¹⁶V. Steinberg, J. Fineberg, E. Moses, and I. Rehberg, *Physica (Amsterdam)* **37D**, 359 (1989).

¹⁷I. Mutabazi, C. Normand, H. Peerhossaini, and J. E. Wesfreid, *Phys. Rev. A* **39**, 763 (1989).

¹⁸L. Gil and J. Lega, in *Propagation in Systems Far from Equilibrium* (Ref. 2), p. 164.

¹⁹A. Joets and R. Ribotta, *J. Phys. (Paris), Colloq.* **50**, C3-171 (1989).

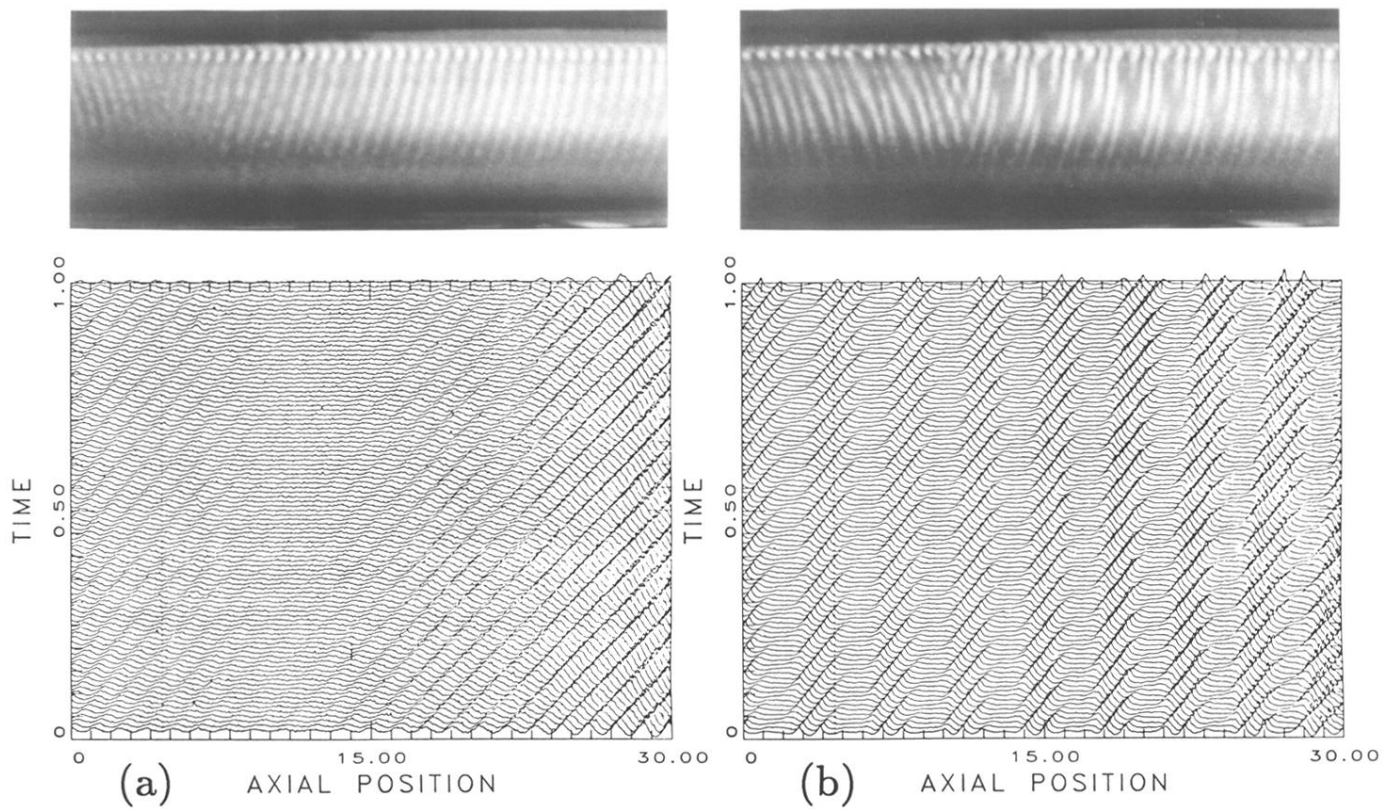


FIG. 2. Photographs of the traveling-roll patterns viewed from the front face (the top of each view being a free horizontal surface) and their space-time diagrams: (a) traveling-inclined-roll pattern near threshold at $R_i=263$ and $R_o=0$. (b) Short-wavelength (~ 3 -roll) -modulation pattern at $R_i=303$ and $R_o=0$.